

Measurements of endothelial cell-to-cell and cell-to-substrate gaps and micromechanical properties of endothelial cells during monocyte adhesion

Noriyuki Kataoka*^{†‡}, Kanso Iwaki[§], Ken Hashimoto*[¶], Seiichi Mochizuki*, Yasuo Ogasawara*, Masaaki Sato^{||}, Katsuhiko Tsujioka[¶], and Fumihiko Kajiya*[†]

Departments of *Medical Engineering and [¶]Physiology, Kawasaki Medical School, 577 Matsushima, Kurashiki, Okayama 701-0192, Japan; [†]Department of Cardiovascular Physiology, Okayama University Graduate School of Medicine and Dentistry, 2-5-1 Shikata, Okayama, Okayama 700-8558, Japan; [§]Fujisaki Institute, Hayashibara Biochemical Laboratories, Inc., 675-1 Fujisaki, Okayama, Okayama 702-8006, Japan; and ^{||}Graduate School of Mechanical Engineering, Tohoku University, 01 Aoba, Aramaki, Aoba-ku, Sendai, Miyagi 980-8579, Japan

Communicated by Ivar Giaever, Rensselaer Polytechnic Institute, Troy, NY, September 30, 2002 (received for review February 22, 2002)

The interaction between monocytes and endothelial cells is considered to play a major role in the early stage of atherosclerosis, and the involved endothelial cell micromechanics may provide us with important aspects of atherogenesis. In the present study, we evaluated (i) the endothelial cell-to-cell and cell-to-substrate gaps with the electric cell-substrate impedance sensing system, which can detect the nanometer order changes of cell-to-cell and cell-to-substrate distances separately, and (ii) the endothelial cell micromechanical properties with an atomic force microscope after application of monocytes to endothelial cells. Application of monocytic THP-1 cells to IL-1 β -stimulated human umbilical vein endothelial cells immediately decreased the electrical resistance of the endothelial cell-to-substrate (increase of the cell-to-substrate gap), whereas the endothelial cell-to-cell resistance (cell-to-cell gap) did not change. The elastic modulus of the endothelial cells decreased after 2-h monocyte application, indicating an increase of endothelial cell deformability. In conclusion, the interaction of the monocytes to the endothelial cells reduced the adhesiveness to the substrate and increased the deformability of endothelial cells. These changes in the adhesiveness and the deformability may facilitate migration of monocytes, a key process of atherogenesis in the later stage.

At the early stage of atherosclerosis, an aggregation of lipid-rich macrophages that were derived from monocytes was observed in the intima (1). Adhesion of monocytes to the arterial endothelial cells and their migration into the arterial intima are the earliest key events in atherogenesis (1). Previous studies demonstrated that leukocytes could migrate throughout the endothelial monolayer via not only paracellular but also transcellular pathways *in vivo* and *in vitro* (2–5). The endothelial cell micromechanics that are involved in endothelial cell micromotion and the mechanical properties of endothelial cells may be key factors in these processes. Earlier studies reported the importance of adhesion molecules in the adhesion and migration of monocytes to endothelial cells (6, 7). We previously demonstrated that the adhesion of monocytes to human umbilical vein endothelial cells (HUVEC) induces the decrease in the amount of focal adhesion kinase (p125^{FAK}) with reduction of the density of F-actin stress fibers in HUVEC (8). These results suggest that the adhesion of monocytes induces changes of the adhesiveness of endothelial cells to the substrate and the mechanical properties of endothelial cells. However, the accompanying micromechanics and micromotion of endothelial cells were little understood.

For the micromotion measurement of the cultured cells, Giaever and Keese (9) developed a morphological biosensor, the electric cell-substrate impedance sensing (ECIS) system. The advantage of this system is that quantitative estimation of

cell-to-cell and cell-to-substrate distances can be performed separately and in real time. Atomic force microscopy (AFM) is a useful tool for examining mechanical properties of cells and imaging biological tissues such as cells, proteins, and DNA. The measurement of mechanical properties of living soft tissue is possible with a nanoindentation technique (10).

In the present study, we applied these two methods, ECIS and AFM, to evaluate the effect of the interaction between monocytes and endothelial cells on endothelial cell micromotion and mechanical properties.

Materials and Methods

Cell Culture. HUVEC were purchased from Cell Systems (Kirkland, WA) and seeded on a gelatin (Sigma)-coated cell culture flask (Becton Dickinson) with CS-C complete medium (Cell Systems). HUVEC were cultured at 37°C in humidified air containing 5% CO₂. The human monocytic cell line THP-1 (Japanese Collection of Research Bioresources, Tokyo) was cultured in RPMI 1640 (Dainippon Pharmaceutical, Osaka) supplemented with 10% FBS (Dainippon Pharmaceutical), 50 μ g/ml kanamycin, and 10 mM Hepes.

Estimation of Cell-to-Cell and Cell-to-Substrate Gaps. HUVEC were seeded on a gelatin-coated cell culture dish (10 mm \times 10 mm for each section; Applied Biophysics, Troy, NY) with a microelectrode (ϕ = 250 μ m) and grown until confluence. HUVEC were then stimulated with human IL-1 β (5 ng/ml; Genzyme) for 6 h and subsequently overlaid with the 20 μ l of culture medium containing THP-1 (1 \times 10⁶ cells/ml). In the ECIS program (Applied Biophysics), there are several kinds of measurement mode: attachment mode (the data are acquired every minute or more), micromotion mode (the data are acquired every few seconds), and frequency scan mode (impedance is measured with variety of frequency). In this study, electrical impedance was measured with the attachment mode of ECIS. The change of impedance is attributed to changes of the resistance in paracellular pathway (R_b) and the resistance between the ventral cell surface and the electrode [α : $\alpha = r(\rho/h)^{0.5}$, where r is the cell radius, ρ is the resistivity of the culture medium, and h is the gap between the cells and the electrode] (9). From the changes of R_b and α , the changes in cell-to-cell and cell-to-substrate gaps were estimated.

Measurement of Mechanical Property. By pressing the AFM cantilever to the cell surface, a force-curve, the relationship between

Abbreviations: HUVEC, human umbilical vein endothelial cells; FAK, focal adhesion kinase; ECIS, electric cell-substrate impedance sensing; AFM, atomic force microscopy.

[†]To whom correspondence should be addressed. E-mail: kataoka@me.kawasaki-m.ac.jp.

the cantilever deflection and its indentation depth, was obtained. In this study, the force-curve of the HUVEC was measured with an AFM (NVB100; Olympus, Tokyo). HUVEC were seeded on a gelatin-coated cell culture dish, and THP-1 was applied in the same protocol as described above. Our previous study indicated that the decrease in p125^{FAK} reached its maximum level 15–30 min after the application of THP-1 to HUVEC and continued up to 2 h, and the F-actin structure changes exhibited a similar time course (8). The changes of F-actin structures were also observed 30 min after the application of THP-1 and continued for at least 2 h. The force-curves were thus measured after 2 h of application of THP-1 to HUVEC. Force-curve measurements were performed in the center region, just above the cell nucleus and the peripheral region of HUVEC. Each measurement was finished within 30 min, because the measurements were performed at room temperature, and some HUVEC were detached from the dish after 1 h at room temperature. Elastic modulus was estimated with the Hertz model that describes the indentation of a homogeneous/semi-infinite elastic material (11), defined as follows:

$$F = \delta^2 \frac{\pi}{2} \frac{E}{(1 - \nu^2)} \tan \alpha,$$

where F is the applied force (calculated from the spring constant multiplied by the cantilever deflection), E is the elastic modulus, ν is the Poisson's ratio assumed to be 0.5 because the cell was considered incompressible, α is the opening angle of the tip of the cantilever, and δ is the indentation depth.

Observation of GFP-Expressed Monocytes. Precise transectional position of monocytes in the endothelial monolayer was observed with a GFP-expressed monocytic cell line donated by Hayashibara Biochemical Laboratories (Okayama, Japan). This cell line was established by Hayashibara Biochemical Laboratories and permanently expresses cytosolic GFP in monocytes. GFP-expressed monocytes were applied to HUVEC that were seeded on a gelatin-coated glass bottom dish (Iwaki, Tokyo) and pretreated with Cell Tracker orange (Molecular Probes) for 30 min. The images of GFP-expressed monocytes and HUVEC were taken by a confocal laser microscope with an incubation system (TCS-NT; Leica Microsystems, Heidelberg, Germany). These images were loaded on a personal computer (PowerMac G4; Apple Computer, Cupertino, CA), and 3D images were reconstructed with the public domain image analyzing program NIH IMAGE (developed at the National Institutes of Health, Bethesda, MD).

Observation of F-Actin and p125^{FAK} in Endothelial Cells. HUVEC were seeded on a gelatin-coated glass bottom dish for observation of F-actin filaments and FAK (p125^{FAK}). THP-1 was applied to HUVEC in the same protocol as described above. After 2 h of application of THP-1, HUVEC were rinsed with PBS (Nissui Seiyaku, Tokyo) and fixed in 2% paraformaldehyde in PBS for 10 min. After fixation, the cells were treated with EDTA (0.2% in PBS; Merck) for ≈ 1 min to remove the adhered THP-1. Subsequently, the cells were permeabilized in 0.1% Triton X-100 (Wako Pure Chemical, Osaka) for 5 min. The cells then were rinsed in PBS and incubated with rhodamine-phalloidin (Molecular Probes) in PBS for 30 min. Finally, the cells were rinsed and mounted over with glycerol/PBS (1:1) with 4% *n*-propylgallate (Wako Pure Chemical) to prevent the fading of fluorescence. In another set of samples, HUVEC were rinsed with PBS and fixed in methanol for 5 min. After fixation, the cells were treated with EDTA for ≈ 1 min. Subsequently, the cells were permeabilized in 0.1% Triton X-100 (Wako Pure Chemical) for 5 min and incubated with anti-p125^{FAK} mAb (1:100 in PBS; Santa Cruz Biotechnology) and FITC-conjugated goat IgG

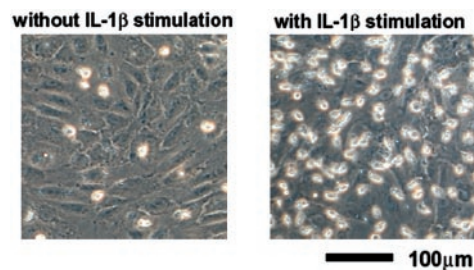


Fig. 1. Photomicrographs of monocytes remaining on the surface of IL-1 β -unstimulated (Left) and stimulated (Right) HUVEC after washing off the nonadherent monocytes.

(1:100 in PBS; Santa Cruz Biotechnology). These samples were observed with a confocal laser microscope (TCS-NT; Leica Microsystems).

Statistics. Paired (analysis for changes of Rb and α) and unpaired (analysis for changes of the total impedance and the elastic modulus) Student's t tests were performed to determine the significance of differences in comparison of the experimental groups. All data are expressed as means \pm SD, and differences are considered to be significant when $P < 0.05$.

Results

Fig. 1 shows the photomicrographs of monocytes that remained on the surface of IL-1 β -unstimulated and stimulated HUVEC after washing off the nonadherent monocytes. After 2 h of application of monocytes, the adhesion monocytes to HUVEC were confirmed. Two or three monocytes adhered per IL-1 β -stimulated HUVEC. In contrast, fewer monocytes adhered on the surface of the unstimulated HUVEC.

Typical traces of the normalized total electrical impedance of the IL-1 β -stimulated and unstimulated HUVEC after application of monocytes are shown in Fig. 2. After application of monocytes (indicated as an arrow in Fig. 2) to the IL-1 β -stimulated HUVEC, electrical impedance immediately decreased, whereas that for the unstimulated HUVEC was almost unchanged. The summary of the changes of electrical impedance for the stimulated ($n = 15$, number of samples) and unstimulated ($n = 17$) HUVEC is also shown in Fig. 2. After 30 min of application of monocytes, there was already a statistically significant difference between the two groups.

Fig. 3 is the typical real-time traces of the total, cell-to-substrate and cell-to-cell resistances in the IL-1 β -stimulated HUVEC. Immediately after application of monocytes (time = 0 in Fig. 3) to the IL-1 β -stimulated HUVEC, cell-to-substrate resistance gradually decreased, whereas cell-to-cell resistance was almost unchanged. Summary of the changes of α (cell-to-substrate) and Rb (cell-to-cell) after 1 h of application of monocytes is shown in Fig. 4. α was significantly decreased by $-40.1 \pm 20.1\%$ ($P < 0.05$, $n = 7$), whereas the change in Rb was not significant ($14.9 \pm 50.6\%$, $n = 7$), indicating that the monocyte adhesion caused the increase of the endothelial cell-to-substrate, but not cell-to-cell distance. The unchanged Rb may imply that the morphology of HUVEC remains constant. Accordingly, we measured cell area and perimeter of HUVEC before and after adhesion of monocytes. These parameters are $1,034 \pm 367 \mu\text{m}^2$ and $132 \pm 24 \mu\text{m}$ under control conditions ($n = 20$), and $1,115 \pm 253 \mu\text{m}^2$ and $134 \pm 17 \mu\text{m}$ after adhesion of monocytes ($n = 15$), respectively. There is no statistical significance in the changes of parameters, indicating almost constant morphology of HUVEC after adhesion of monocytes.

Fig. 5 shows the computer-reconstructed 3D images of the GFP-expressed monocytes (green) and HUVEC (red). It is

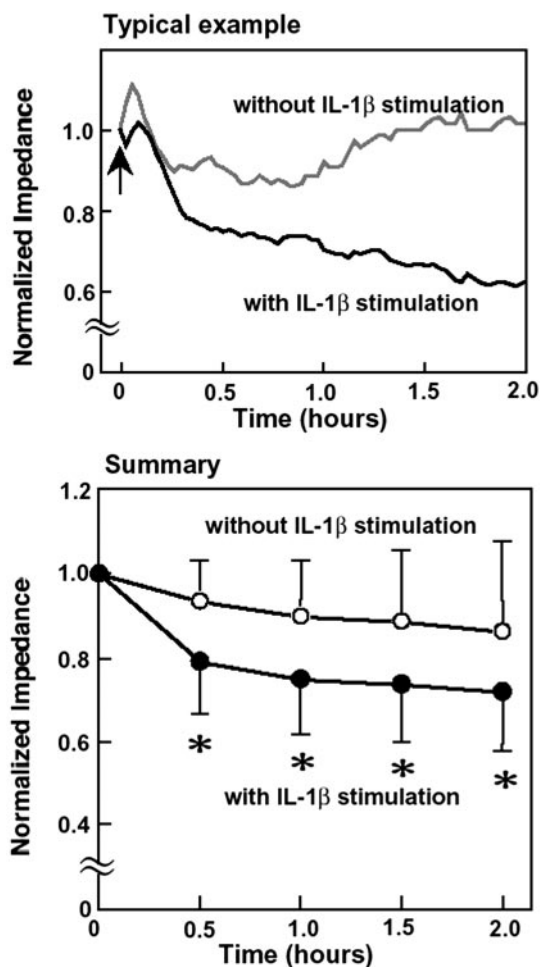


Fig. 2. Typical examples and summary of the total electrical impedance changes of the IL-1 β -stimulated and unstimulated HUVEC after application of monocytes. (Upper) Black line, stimulated HUVEC; gray line, unstimulated HUVEC. Arrow indicates the application of monocytes. (Lower) \circ , Unstimulated HUVEC ($n = 17$); \bullet , stimulated HUVEC, ($n = 15$). *, $P < 0.05$ stimulated HUVEC vs. unstimulated HUVEC.

noticeable that monocytes adhered to the cell surface, but did not migrate into the endothelial monolayer at this stage, indicating that the increase of endothelial cell-to-substrate distance

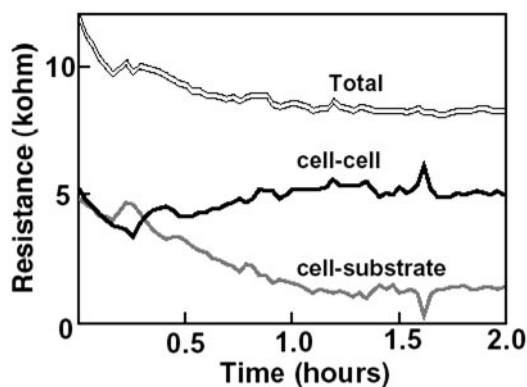


Fig. 3. Typical real-time traces of the total (double line), cell-to-substrate (gray line), and cell-to-cell (black line) resistance in the IL-1 β -stimulated HUVEC.

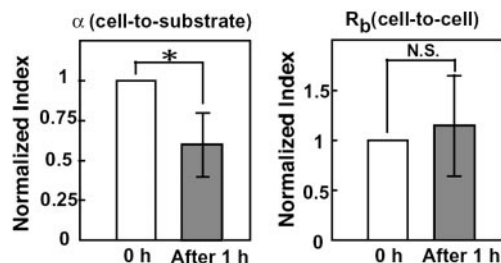
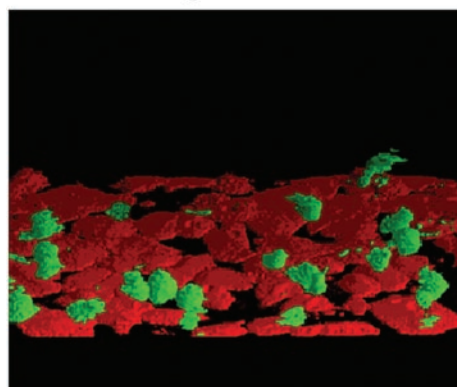


Fig. 4. Summary of the normalized values of α (cell-to-substrate) and R_{β} (cell-to-cell) after 1 h of monocyte application. *, $P < 0.05$; N.S., not significant.

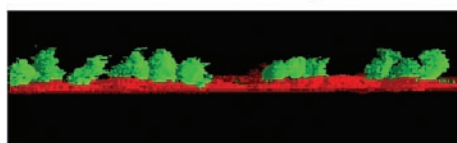
was not caused by the monocytes' migration into the endothelial cell monolayer.

Typical force-curves for the peripheral region of the control HUVEC (without stimulation by IL-1 β) and the monocyte-adhered HUVEC are shown in Fig. 6. The force-curves were well fitted with a parabolic curve ($r^2 = 0.99$). The force-curve for the monocyte-adhered HUVEC shows a smaller slope compared with that of control HUVEC. The changes of the elastic modulus in both the center and peripheral regions are summarized in Fig. 7. Under the control condition, the elastic modulus in the central region (3.0 ± 1.6 kPa, $n = 11$, number of cells) was significantly smaller than that in the peripheral region (6.7 ± 4.3 kPa, $n = 11$). The elastic modulus of the monocyte-adhered HUVEC significantly decreased in both the central (1.5 ± 1.2 kPa, $P < 0.05$ vs. control, $n = 12$) and peripheral regions (2.7 ± 1.9 kPa, $P < 0.05$ vs. control, $n = 12$). We then measured the mechanical property of the monocyte-adhered and unadhered HUVEC in the same dish when monocytes were sparsely applied. The elastic modulus of HUVEC without monocyte adhesion (in the center: 2.7 ± 1.8 kPa, $n = 13$, in the periphery: 7.2 ± 5.6 kPa, $n = 13$) were the same as those under control conditions. The elastic modulus of HUVEC with monocyte adhesion (in the center: 1.6 ± 0.6 kPa,

En-face image



Cross-sectional image



50 μ m

Fig. 5. Computer-reconstructed 3D images of GFP-expressed monocytes (green) and endothelial cells (red) after 2 h of application.

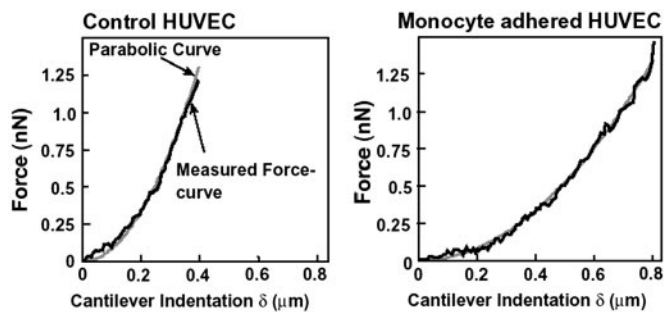


Fig. 6. Typical force-curves for the peripheral region of control (Left) and monocyte-adhered (Right) HUVEC measured with AFM. Black lines, measured force-curve; gray lines, fitted parabolic curve.

$n = 9$, in the periphery: 3.0 ± 1.8 kPa, $n = 9$) were significantly smaller than those of HUVEC without monocyte adhesion in both center and periphery ($P < 0.05$) as shown in Fig. 7. These results demonstrated that HUVEC became softer, i.e., the deformability was increased, after monocyte adhesion and that these changes were substantially triggered by the direct contact between monocytes and endothelial cells.

As we had reported through Western blotting analysis and a microscope equipped with epifluorescence optics (8), we observed the reduction of both F-actin density and p125^{FAK} with a confocal laser microscope as shown in Fig. 8. Before application of monocytes, the F-actin filaments were observed in the center portion as the stress fibers and at the periphery of the cells as the dense peripheral bands. After 2 h of monocyte application, the density of F-actin filaments was reduced in both the center and peripheral regions of the cells. FAK was observed dispersively in the whole cells. After monocyte adhesion, p125^{FAK} was reduced in the whole cells.

Discussion

We directly evaluated the endothelial cell micromechanics affected by the interaction between monocytes and endothelial cells. The main findings are as follows: (i) Application of monocytes to HUVEC immediately decreased the endothelial cell-to-substrate resistance (increase of cell-to-substrate gap), whereas the endothelial cell-to-cell resistance (cell-to-cell gap) was unchanged. (ii) The elastic modulus of HUVEC decreased after 2-h monocyte application.

The decrease of the endothelial cell-to-substrate resistance (increase of cell-to-substrate gap), α , may be closely related with the change of the adhesiveness of endothelial cells to the substrate. We demonstrated that the amount of FAK (p125^{FAK})

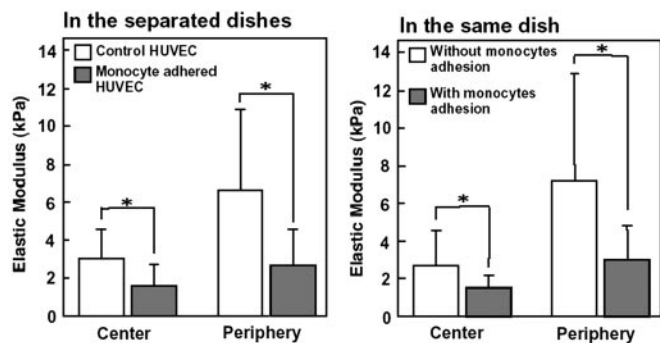


Fig. 7. Elastic modulus of HUVEC measured in the separated dishes (Left; nonapplication and application of monocytes). Elastic modulus of HUVEC with and without monocytes adhesion in the same dish (Right). Open bars, without monocyte adhesion; filled bars, with monocyte adhesion.

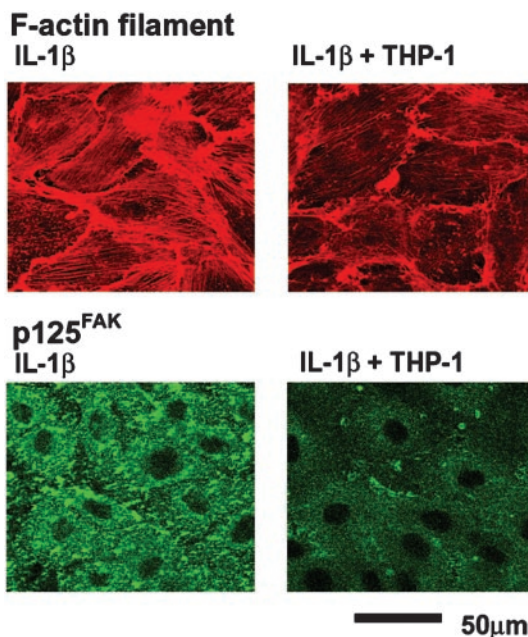


Fig. 8. Photomicrographs of F-actin filaments and p125^{FAK} in HUVEC before and after application of monocytes.

in HUVEC decreased after adhesion of monocytes as shown in Fig. 8. This finding is consistent with our previous study demonstrating the same phenomenon by Western blotting analysis (8). FAK is a kind of tyrosine kinase localized at the focal adhesion complex with several other molecules such as talin, vinculin, and tensin, and it plays a central role in the endothelial cell attachment to the extracellular matrices (12–14). It has been reported that the inhibition of the p125^{FAK} function blocked the formation of focal contacts (13). In addition, the loss of p125^{FAK} has been reported to be a prerequisite for cell detachment (15). Noiri *et al.* (16) reported that the adhesiveness of endothelial cells to substrate was reduced by the NO donor sodium nitroprusside, and the reduction of focal contacts agreed well with the decrease of α , the parameter of cell-to-substrate resistance in the ECIS system (16). Therefore, the decrease of α after application of monocytes in the present study may indicate the rearrangement of the focal contacts of endothelial cells. The cellular adhesiveness is probably decreased during the morphological change of the cells. Because endothelial cells need to change their shape dynamically during monocyte transendothelial migration, the endothelial cells may need to reduce their adhesiveness in the process of monocyte adhesion.

Monocyte adhesion resulted in the decrease in the elastic modulus of HUVEC. The changes of the elastic modulus of HUVEC after adhesion of monocytes are considered to be caused by the reduction of F-actin filaments. Sato *et al.* (17) reported that the F-actin structure is closely related to the mechanical properties of endothelial cells. After exposure to shear stress, thick F-actin stress fibers were formed in cultured bovine endothelial cells, and cells became stiffer. As shown in Fig. 8, F-actin filaments are densely composed in the peripheral region of HUVEC before adhesion of monocytes. The change of the elastic modulus in this region after adhesion of monocytes may be directly caused by the reduction of F-actin filaments. F-actin stress fibers generate tension inside cells and play an important role in forming their morphology and mechanical properties (18). Reduction of F-actin stress fibers thus decreases the tension inside HUVEC, resulting in the decrease of the elastic modulus of the cells. Accordingly, the change of the

mechanical property in the center region is also considered to be caused by changes of F-actin structures. The decrease of the elastic modulus in the peripheral region (by 58%) is larger than that in the center region (by 43%). This regional difference of elastic modulus within a cell may facilitate the emigration of monocytes through the paracellular pathway.

Recently, Wang *et al.* (19) investigated the stiffness of tumor necrosis factor α -stimulated pulmonary microvascular endothelial cells after neutrophil adhesion with a magnetic beads twisting technique and reported that neutrophil adhesion induces the increase in both the stiffness and the F-actin filaments of the endothelial cell. Other investigators also reported that leukocyte adhesion increases F-actin filaments in endothelial cells (20, 21). These results are in contrast to the results in the present study. The first possible explanation for the differences may be the functional differences between monocyte and neutrophil. Kim *et al.* (22) reported that minimally oxidized low-density lipoprotein treatment to endothelial cells induced the adhesion of monocytes but not neutrophils. This finding may be important clinically, because leukocytes that are frequently observed in the atherosclerotic regions are monocytes/macrophages and lymphocytes *in vivo* (23). The other possibility may be the differences in the experimental conditions, such as cytokines used to stimulate endothelial cells and the extracellular matrices used to coat the cell culture dish. Both IL-1 β and tumor necrosis factor α increase the expression of adhesion molecules to leukocytes on the endothelial cell surface (7). The disappearance of the dense peripheral bands and the formation of stress fibers in endothelial cells induced by tumor necrosis factor α stimulation itself were reported by Wang *et al.* (19) and Molony and Armstrong (24), whereas IL-1 β did not cause any appreciable changes of the F-actin structures (8), elastic modulus (see Fig. 7), and the impedance values [$12,123 \pm 1,585$ (ohm) without stimulation and $12,405 \pm 1,906$ (ohm) with stimulation]. Thus, cytokine stimulation may affect endothelial cell structure differently. Fibronectin (19, 25), collagen (20), and gelatin (ref. 8, this study) were widely used to coat the cell culture dish. The cellular receptors for extracellular matrix proteins belong to the integrin superfamily (26). The attachment of endothelial cells to artificial surfaces under flow condition (27), the cytoskeletal organization in endothelial cells (28), and the adhesion force between the integrins and their ligands (29) strongly depend on the type of extracellular matrix. Therefore, the extracellular matrices that were used to coat the cell culture dish probably affect the endothelial cell responses to adhesion of leukocyte.

It is well known that atherosclerotic lesions tend to localize at the arterial branch and curved sites (30). In these regions, the endothelial cell shape is round (31, 32), the density of F-actin filaments is lower than those in other regions (33), and monocyte

adhesion and migration were frequently observed (34). The increased shear stress in the contralateral common carotid artery to the ligated common carotid artery increases the elongation of the endothelial cells and F-actin filaments and decreases monocyte adhesion and migration (35). Furthermore, the relationship between the mechanical properties and the endothelial cell shape, i.e., softer properties of the rounded endothelial cells with less F-actin stress fibers compared with the elongated cells, was reported not only in the cultured cells (36) but also in the cells in the fresh vascular segments (37). The monocyte transmigration frequently occurred in the region where the endothelial cells are less elongated and softer with the fewer F-actin filaments. Our results demonstrated that the monocyte adhesion itself induces the decrease of the F-actin structures and the increase of the deformability of endothelial cells, because we observed adhesion of monocytes to endothelial cells but not transendothelial migration as shown in Fig. 5. This finding may suggest that the change in resistance (ECIS) was caused by the changes in α . We speculate that these micromechanical changes may facilitate the migration of monocytes in the later stage.

Adhesion molecules, such as E-selectin, P-selectin, vascular cell adhesion molecule 1, and intercellular adhesion molecule-1, were proposed as the key molecules that affect the signal transduction pathway in endothelial cells and induce the functional changes of endothelial cells in the interaction with leukocytes (20, 38). In the present study, we showed that monocyte adhesion directly affects the mechanical properties of endothelial cells (Fig. 7). We thus consider that adhesion molecules participating in monocyte adhesion may play major roles in the intracellular signaling pathway. However, we do not exclude the other unknown mechanisms. Additional experiments to determine the signaling mechanism, which induces the functional change of endothelial cells, are needed.

In conclusion, using ECIS and AFM, we demonstrated that monocyte adhesion reduces the adhesiveness of endothelial cells to the substrate and increases the deformability of endothelial cells. The adhesion of monocytes may play a pivotal role in the initial stage of atherogenesis by affecting the signal-transduction pathway in endothelial cells and by inducing the reconstruction of the focal adhesion complex and actin filaments, resulting in the facilitated migration of monocytes.

We thank Dr. Ivar Giaever (Physics Department, Rensselaer Polytechnic Institute and Applied BioPhysics), Dr. Charles R. Keese (Department of Biology, Rensselaer Polytechnic Institute and Applied BioPhysics), and Dr. Natacha DePaola (Biomedical Engineering Department, Rensselaer Polytechnic Institute) for their valuable support, suggestions, and comments. This work was supported in part by research grants from the Ministry of Education, Science, and Culture, Japan (Grants-in-Aids for Scientific Research B nos. 12558114 and 12480270).

1. Ross, R. (1993) *Nature* **362**, 801–809.
2. Migliorisi, G., Folkes, E., Pawlowski, N. & Cramer, E. B. (1987) *Am. J. Pathol.* **127**, 157–167.
3. Burns, A. R., Walker, D. C., Brown, E. S., Thurmon, L. T., Bowden, R. A., Keese, C. R., Simon, S. I., Entman, M. L. & Smith, C. W. (1997) *J. Immunol.* **159**, 2893–2903.
4. Feng, D., Nagy, J. A., Pyne, K., Dvorak, H. F. & Dvorak, A. M. (1998) *J. Exp. Med.* **187**, 903–915.
5. Allport, J. R., Muller, W. A. & Lusinskas, F. W. (2000) *J. Cell Biol.* **148**, 203–216.
6. Butcher, E. C. (1991) *Cell* **67**, 1033–1036.
7. Springer, T. A. (1994) *Cell* **76**, 301–314.
8. Iwaki, K., Ohashi, K., Ikeda, M., Tsujioka, K., Kajiya, F. & Kurimoto, M. (1997) *J. Biol. Chem.* **272**, 20665–20670.
9. Giaever, I. & Keese, C. R. (1991) *Proc. Natl. Acad. Sci. USA* **88**, 7896–7900.
10. Weisenhorn, A. L., Khorsandi, M., Kasas, S., Gotzos, V. & Butt, H.-J. (1993) *Nanotechnology* **4**, 106–113.
11. Radmacher, M., Fritz, M., Kacher, C. M., Cleveland, J. P. & Hansma, P. K. (1996) *Biophys. J.* **70**, 556–567.
12. Schaller, M. D., Borgman, C. A., Cobb, B. S., Vines, R. R., Reynolds, A. B. & Parsons, J. T. (1992) *Proc. Natl. Acad. Sci. USA* **89**, 5192–5196.
13. Richardson, A. & Parsons, J. T. (1996) *Nature* **380**, 538–540.
14. Burridge, K., Turner, C. E. & Romer, L. H. (1992) *J. Cell Biol.* **119**, 893–903.
15. Fincham, V. J., Wyke, J. A. & Frame, M. C. (1995) *Oncogene* **10**, 2247–2252.
16. Noiri, E., Lee, E., Testa, J., Quigley, J., Colflesh, D., Keese, C. R., Giaever, I. & Goligorsky, M. S. (1998) *Am. J. Physiol.* **274**, C236–C244.
17. Sato, M., Levesque, M. J. & Nerem, R. M. (1987) *Arteriosclerosis* **7**, 276–286.
18. Ingber, D. E. (1993) *J. Cell Sci.* **104**, 613–627.
19. Wang, Q., Chiang, E. T., Lim, M., Lai, J., Rogers, R., Janmey, P. A., Shepro, D. & Doerschuk, C. M. (2001) *Blood* **97**, 660–668.
20. Lorenzon, P., Vecile, E., Nardon, E., Ferrero, E., Harlan, J. M., Tedesco, F. & Dobrina, A. (1998) *J. Cell Biol.* **142**, 1381–1391.
21. Saito, H., Minamiya, Y., Kitamura, M., Saito, S., Enomoto, K., Terada, K. & Ogawa, J. (1998) *J. Immunol.* **161**, 1533–1540.
22. Kim, J. A., Territo, M. C., Wayner, E., Carlos, T. M., Parhami, F., Smith, C. W., Haberland, M. E., Fogelman, A. M. & Berliner, J. A. (1994) *Arterioscler. Thromb.* **14**, 427–433.

23. Stary, H. C., Chandler, A. B., Dinsmore, R. E., Fuster, V., Glagov, S., Insull, W., Jr., Rosenfeld, M. E., Schwartz, C. J., Wagner, W. D. & Wissler, R. W. (1995) *Arterioscler. Thromb. Vasc. Biol.* **15**, 1512–1531.
24. Molony, L. & Armstrong, L. (1991) *Exp. Cell Res.* **196**, 40–48.
25. Wojciak-Stothard, B., Williams, L. & Ridley, A. J. (1999) *J. Cell Biol.* **145**, 1293–1307.
26. Hynes, R. O. (1992) *Cell* **69**, 11–25.
27. Ivarsson, B. L., Cambria, R. P., Megerman, J. & Abbott, W. M. (1989) *J. Surg. Res.* **47**, 203–207.
28. Pratt, B. M., Harris, A. S., Morrow, J. S. & Madri, J. A. (1984) *Am. J. Pathol.* **117**, 349–354.
29. Lehenkari, P. P. & Horton, M. A. (1999) *Biochem. Biophys. Res. Commun.* **259**, 645–650.
30. DeBakey, M. E., Lawrie, G. M. & Glaeser, D. H. (1985) *Ann. Surg.* **201**, 115–131.
31. Garrity, R. G., Richardson, M., Sommer, J. B., Bell, F. P. & Schwartz, C. J. (1977) *Am. J. Pathol.* **98**, 313–334.
32. Okano, M. & Yoshida, Y. (1992) *Trans. ASME J. Biomech. Eng.* **114**, 301–308.
33. Kim, D. W., Langille, B. L., Wong, M. K. K. & Gotlieb, A. I. (1989) *Circ. Res.* **64**, 21–31.
34. Kolpakov, V., Polishchuk, R., Bannykh, S., Rekhter, M., Solovjev, P., Romanov, Y., Tararak, E., Antonov, A. & Mironov, A. (1996) *Atherosclerosis* **122**, 173–189.
35. Walpole, P. L., Gotlieb, A. I. & Langille, B. L. (1993) *Am. J. Pathol.* **142**, 1392–1400.
36. Sato, M., Nagayama, K., Kataoka, N., Sasaki, M. & Hane, K. (2000) *J. Biomech.* **33**, 127–135.
37. Miyazaki, H. & Hayashi, K. (1999) *Med. Biol. Eng. Comp.* **37**, 530–536.
38. Etienne, S., Adamson, P., Greenwood, J., Strosberg, A. D., Cazaubon, S. & Couraud, P. O. (1998) *J. Immunol.* **161**, 5755–5761.